AFRL-AFOSR-VA-TR-2018-0329

Gradient based optimization and control of chaotic multidisciplinary systems via Least Squares Shadowing adjoint method

Qiqi Wang
MASSACHUSETTS INSTITUTE OF TECHNOLOGY

08/10/2018
Final Report

Air Force Research Laboratory
AF Office Of Scientific Research (AFOSR)/ RTA2
Arlington, Virginia 22203
Air Force Materiel Command

REPORT DOCUMENTATION PAGE

Form Approved
OMB No. 0704-0188

1. REPORT DATE *(DD-MM-YYYY)*	**2. REPORT TYPE**	**3. DATES COVERED** *(From - To)*
08/08/2018	Final Report	01/01/2015-12/31/2017

4. TITLE AND SUBTITLE
Gradient based optimization and control of chaotic multidisciplinary systems via Least Squares Shadowing adjoint method

5a. CONTRACT NUMBER
FA9550-15-1-0072

5b. GRANT NUMBER

5c. PROGRAM ELEMENT NUMBER

6. AUTHOR(S)
Qiqi Wang

5d. PROJECT NUMBER

5e. TASK NUMBER

5f. WORK UNIT NUMBER

7. PERFORMING ORGANIZATION NAME(S) AND ADDRESS(ES)
MIT
77 Massachusetts Ave, Cambridge, MA 02139

8. PERFORMING ORGANIZATION REPORT NUMBER

9. SPONSORING/MONITORING AGENCY NAME(S) AND ADDRESS(ES)
Air Force Office of Scientific Research
875 N. Randolph St, Ste 325
Arlington, VA 22203

10. SPONSOR/MONITOR'S ACRONYM(S)

11. SPONSOR/MONITOR'S REPORT NUMBER(S)

12. DISTRIBUTION/AVAILABILITY STATEMENT
DISTRIBUTION A: Distribution approved for public release.

13. SUPPLEMENTARY NOTES

14. ABSTRACT

This project has successfully developed the Least Squares Shadowing method for computing sensitivity gradients for optimizing the long-time behavior of chaotic dynamical systems, such as many unsteady flows. The Non-Intrusive-Least-Squares-Shadowing (NILSS) method has been developed theoretically. Its application to several computational fluid dynamics problems has been demonstrated.

15. SUBJECT TERMS

16. SECURITY CLASSIFICATION OF:			**17. LIMITATION OF ABSTRACT**	**18. NUMBER OF PAGES**	**19a. NAME OF RESPONSIBLE PERSON**
a. REPORT	**b. ABSTRACT**	**c. THIS PAGE**			**19b. TELEPHONE NUMBER** *(Include area code)*

INSTRUCTIONS FOR COMPLETING SF 298

1. REPORT DATE. Full publication date, including day, month, if available. Must cite at least the year and be Year 2000 compliant, e.g. 30-06-1998; xx-06-1998; xx-xx-1998.

2. REPORT TYPE. State the type of report, such as final, technical, interim, memorandum, master's thesis, progress, quarterly, research, special, group study, etc.

3. DATE COVERED. Indicate the time during which the work was performed and the report was written, e.g., Jun 1997 - Jun 1998; 1-10 Jun 1996; May - Nov 1998; Nov 1998.

4. TITLE. Enter title and subtitle with volume number and part number, if applicable. On classified documents, enter the title classification in parentheses.

5a. CONTRACT NUMBER. Enter all contract numbers as they appear in the report, e.g. F33315-86-C-5169.

5b. GRANT NUMBER. Enter all grant numbers as they appear in the report. e.g. AFOSR-82-1234.

5c. PROGRAM ELEMENT NUMBER. Enter all program element numbers as they appear in the report, e.g. 61101A.

5e. TASK NUMBER. Enter all task numbers as they appear in the report, e.g. 05; RF0330201; T4112.

5f. WORK UNIT NUMBER. Enter all work unit numbers as they appear in the report, e.g. 001; AFAPL30480105.

6. AUTHOR(S). Enter name(s) of person(s) responsible for writing the report, performing the research, or credited with the content of the report. The form of entry is the last name, first name, middle initial, and additional qualifiers separated by commas, e.g. Smith, Richard, J, Jr.

7. PERFORMING ORGANIZATION NAME(S) AND ADDRESS(ES). Self-explanatory.

8. PERFORMING ORGANIZATION REPORT NUMBER. Enter all unique alphanumeric report numbers assigned by the performing organization, e.g. BRL-1234; AFWL-TR-85-4017-Vol-21-PT-2.

9. SPONSORING/MONITORING AGENCY NAME(S) AND ADDRESS(ES). Enter the name and address of the organization(s) financially responsible for and monitoring the work.

10. SPONSOR/MONITOR'S ACRONYM(S). Enter, if available, e.g. BRL, ARDEC, NADC.

11. SPONSOR/MONITOR'S REPORT NUMBER(S). Enter report number as assigned by the sponsoring/ monitoring agency, if available, e.g. BRL-TR-829; -215.

12. DISTRIBUTION/AVAILABILITY STATEMENT. Use agency-mandated availability statements to indicate the public availability or distribution limitations of the report. If additional limitations/ restrictions or special markings are indicated, follow agency authorization procedures, e.g. RD/FRD, PROPIN, ITAR, etc. Include copyright information.

13. SUPPLEMENTARY NOTES. Enter information not included elsewhere such as: prepared in cooperation with; translation of; report supersedes; old edition number, etc.

14. ABSTRACT. A brief (approximately 200 words) factual summary of the most significant information.

15. SUBJECT TERMS. Key words or phrases identifying major concepts in the report.

16. SECURITY CLASSIFICATION. Enter security classification in accordance with security classification regulations, e.g. U, C, S, etc. If this form contains classified information, stamp classification level on the top and bottom of this page.

17. LIMITATION OF ABSTRACT. This block must be completed to assign a distribution limitation to the abstract. Enter UU (Unclassified Unlimited) or SAR (Same as Report). An entry in this block is necessary if the abstract is to be limited.

Final Report

PM: Fariba Fahroo

PI: Qiqi Wang

Institution: Massachusetts Institute of Technology

Project Title: Gradient based optimization and control of chaotic multidisciplinary systems via Least Squares Shadowing adjoint method

AFOSR Award Number: FA9550-15-1-0072

Project description and goals

This research project serves air force by addressing engineering problems important to air force. These problems include turbulent flows and other nonlinear multi-disciplinary, multi-physics phenomena. Air force can significantly benefit from efficient computation tools for design optimization and optimal control of these problems. Such tools have proven useful in many aerodynamics problems. However, they are not yet available for many problems important to air force, if modeling these problem require long time simulation of nonlinear and chaotic dynamics. These problems include chaotic aeroelastic limit cycle oscillations and high fidelity Large Eddy Simulations. They defy traditional methods, e.g., the adjoint method, because the sensitivity that defines chaos leads to exponential growth of linearized equation. This prevents application of traditional sensitivity analysis method to long time averaged quantities of interest, e.g., aerodynamic performance and structure fatigue.

The proposed research aims to benefit air force by enabling efficient design optimization and optimal control of these air force-relevant problems. Achieving this goal requires overcoming the failure suffered by traditional sensitivity analysis methods in chaotic nonlinear simulations. This project aims to overcome this challenge using Least Squares Sensitivity Analysis, a new computational method being developed by the PI. This new method will be extended to complex chaotic flows and flow structure interaction problems. Goals include extended mathematical theory, new algorithms, new software and new application. The proposed work will be the world's first sensitivity analysis of mean quantities in complex, chaotic flow-structure interactions. The resulting computational tool for design, optimization and control of large scale, chaotic dynamical systems will be innovative algorithm and software product. The military significance and commercial value of the product include design optimization of flexible structures in extreme environments, and other applications including cooling and combustion in hypersonic vehicles.

Technical Accomplishments

The goal of this proposal is to investigate efficient approaches to optimize long-time behavior of parameterized chaotic dynamical systems. Such optimization problems can be formulated mathematically as follows:

$$\min_s \langle J \rangle(s) \coloneqq \lim_{T\to\infty} \frac{1}{T} \int_0^T J(u(t), s)dt \ , \qquad where \qquad \frac{du}{dt} = f(u(t), s)$$

Here, $u(t)$ is the time-dependent state of the dynamical system. It satisfies a differential equation parameterized by s. In turbulent flows, for example, $u(t)$ represent the entire unsteady flow field. It satisfies the Navier-Stokes equation, the parameter of which can be the geometry and boundary conditions. J, a function of the state represent the quantity of interest, e.g., the aerodynamic drag. The final objective function $\langle J \rangle$ to be minimized is the infinite-long-time averaged quantity of interest. In a chaotic system in statistically steady-state, the quantity of interest commonly behave like a stationary stochastic time series. An example is given in Figure 1.

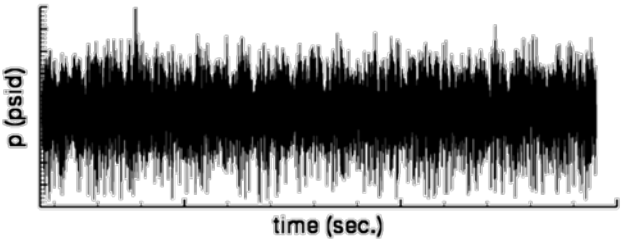

Figure 1. The unsteady pressure of a buffeting launch vehicle [Brauckmann 2015].

When the system has many parameters, i.e., when s is a high dimensional vector, gradient-based optimization has proven to be an effective way to solve this problem. This method computes the gradient of $\langle J \rangle$ with respect to s. This gradient then drives an optimization routine such as steepest descent or quasi-Newton. This gradient-based approach has found many applications in aerodynamic optimization.

It is difficult to compute the gradient of $\langle J \rangle$ with respect to s when $\langle J \rangle$ is the infinitely-long time average of an apparently stochastic time series. This difficulty can be illustrated with a simple example. Consider $J_1, J_2, \ldots$ be independent random variables, each following an identical uniform distribution between 0 and a parameter s. What is the derivative of $\langle J \rangle$, the infinitely-long-time average of $J_1, J_2, \ldots$, with respect to s? Analytically, we know from the law of large number that the $\langle J \rangle = s/2$. Thus, its derivative to s is ½. If such analytics are not available, as in most long-time averages of dynamical systems, we need to compute the derivative by performing finite difference on sample averages, which is noisy.

Figure 1 uses a IPython Notebook, available at https://colab.research.google.com/drive/1mCr82dFWKsIZ4azvbHM6-x17wdwiWsGW , to illustrate how much the noise affects the finite difference result. Using 1000 samples and a step size of 0.001, one obtains a derivative remarkably different from the analytical value of ½. Decreasing the finite difference step size, which normally would increase the accuracy of finite difference results, actually further undermines the accuracy of the result. The accuracy is improved only by increasing the sample size, albeit very slowly. An unremarkable 2% accuracy requires 100 million samples, the computation cost of which is acceptable only in extremely simple cases like this one. The same difficulty plague gradient computation for long-time-averaged quantities in chaotic dynamical systems, such as the one illustrated in Figure 1. In such problems, weeks of computation on thousands of processors would be required to generate the equivalent of 1000 independent samples.

```
[1]  from numpy import *

     def sampleMean(s, N):
         J = random.rand(N) * s
         return J.mean()

     def finiteDiff(s, eps, N):
         return (sampleMean(1+eps, N) - sampleMean(1-eps, N)) / (2*eps)
```

```
[2]  print(finiteDiff(s=1, eps=1E-3, N=1000))
     print(finiteDiff(s=1, eps=1E-5, N=1000))
     print(finiteDiff(s=1, eps=1E-7, N=1000))
```

```
0.13707842710114493
189.20601203357145
150861.84759108446
```

```
[3]  print(finiteDiff(s=1, eps=1E-3, N=10000))
     print(finiteDiff(s=1, eps=1E-3, N=100000))
     print(finiteDiff(s=1, eps=1E-3, N=1000000))
     print(finiteDiff(s=1, eps=1E-3, N=10000000))
     print(finiteDiff(s=1, eps=1E-3, N=100000000))
```

```
-1.2350362737525988
-0.5597132951332684
0.8669407781446703
0.5598612388433288
0.5129419116591538
```

Figure 2. Accuracy of finite difference on the mean of stochastic time series.

To illustrate the impact of the sampling error on sensitivities computed with finite-differences, we use the Lorenz attractor, a simple model of chaotic fluid convection between a hot plane below and a cold plane above. The objective is defined as a function of the convective heat transfer, and the design variable is the Rayleigh number *r*, a non-dimensionalized temperature difference between the hot and cold planes. Figure 2.3 shows the dependence of the objective function on the design parameter. The objective function in different subfigures is computed using simulations of the various lengths of time windows.

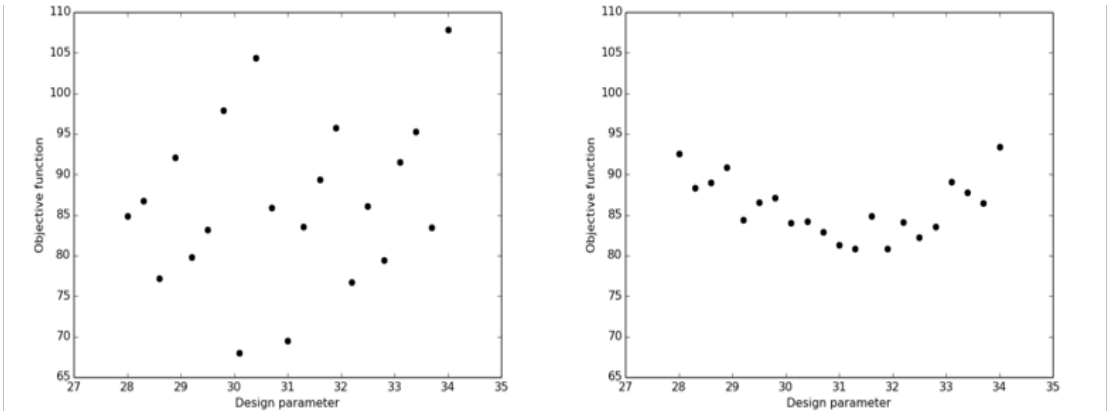

(a) T = 5 (b) T = 50

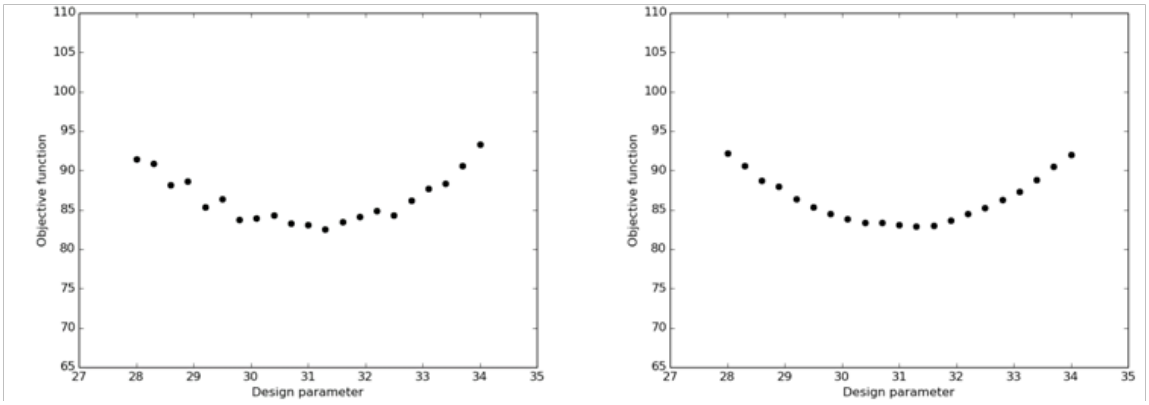

(c) T = 500 (d) T = 5,000

Figure 3. Time Average of $(z-28)^2$ in the Lorenz Attractor Over Four Different Time Spans T, as a Function of r, for b = 8/3 and s=10.

Figure 2.3(a) plots the objective function averaged over a time window of 5-time units. Note that the longest time scale of the dynamics of the Lorenz attractor is about 1 time unit. Despite being averaged over a time window several times longer than the longest time scale of the system, the computed statistic shows no discernible trend. The noise due to sampling error is so large that it is impossible to infer how the objective function depends on the parameter. To reduce the sampling error, one can increase the averaging length, as shown in Figures 2.3 (b), (c), and (d). These figures indicate that there is an apparent minimum of the statistic. Reducing sampling error by a factor of 10 would require increasing the window size by a factor of 100 [7]. For high-fidelity simulations, the computation time quickly becomes infeasible.

The slow decaying sampling error has significant adverse effects on many optimization algorithms. Surrogate-based optimization, for example, should take into account the noise in the objective function due to sampling error [8]. Gradient-based optimization, suitable when there are many design parameters, also faces challenges from the sampling error. These optimization algorithms require computing the gradient of the objective function, either using finite difference or using analytical methods such as the tangent or adjoint method. Both finite difference and analytical methods have

difficulties dealing with the sampling error when the quantity of interest is a computed statistic of a chaotic dynamical system.

How finite difference method suffers from the sampling error can be understood from Figure 2.3. Finite difference approximates a derivative by selecting two adjacent design points, evaluating their objective functions, and dividing their difference by the distance between the design points. When both objective functions are polluted by sampling errors, the resulting derivative, a slope between nearby points in Figure 2.3, is polluted by a larger error. The error is equal to the sum of the sampling errors divided by the distance between the design points. Because the design points in a finite difference must be adjacent to an accurate Taylor series approximation, the resulting error in the gradient can be overwhelming. To obtain reasonably accurate finite difference derivatives, multiple very long time averages, such as 5000 times the longest chaotic timescale, as in Figure 2.3(d), must be used.

While the finite difference method errs, a naive application of analytical methods, including the adjoint method, fails completely. The adjoint method calculates gradients by tracing backwards through all the elementary operations in the solver, applying chain rule to each operation. It generates gradients that should agree with, up to round off error, a finite difference calculation of infinitesimal step size. It is not surprising that the adjoint method suffers from the same difficulties. The adjoint solution diverges when the simulation is chaotic. The gradient computed from the adjoint solution is the gradient of an approximation that equals the objective function plus a sampling error. This sampling error decorrelates under little changes of the design variables. Even when the sampling error is small, its gradient can be significant. The gradient computed is polluted by the gradient of the sampling error. It can be orders of magnitude larger than the correct gradient and is useless for optimization. Figure 3 shows some diverging adjoint solutions of chaotic flow simulations in the literature.

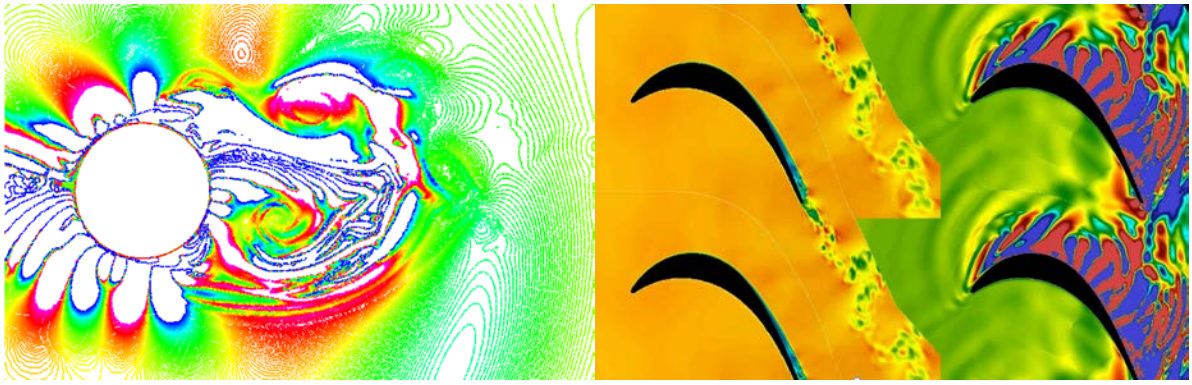

Figure 4. Diverging adjoint solutions. Left: Barth (2014). Right: Diosady et al. (2016).

The Least Squares Shadowing (LSS) method has been developed to address the challenge of performing analytical sensitivity analysis to statistics in chaotic simulations. Figure 5 uses red line segments to visualize the sensitivity derivatives computed using this method. The method works by replacing the initial value problem, which is employed in the derivation of the conventional tangent and adjoint method but is ill-conditioned in chaotic dynamical systems, with the well-conditioned Least Squares Shadowing problem [10]. The solution to the Least Squares Shadowing problem approximates the gradient of the infinitely-long-time averaged statistic, as opposed to the corrupted gradient of the finite-time average. As can be seen in Figure 5, accurate sensitivity derivatives can be computed with a

relatively short time window. The computed gradient, therefore, can be used to efficiently optimize physical quantities of interest describing the long-time behavior of chaotic dynamical systems.

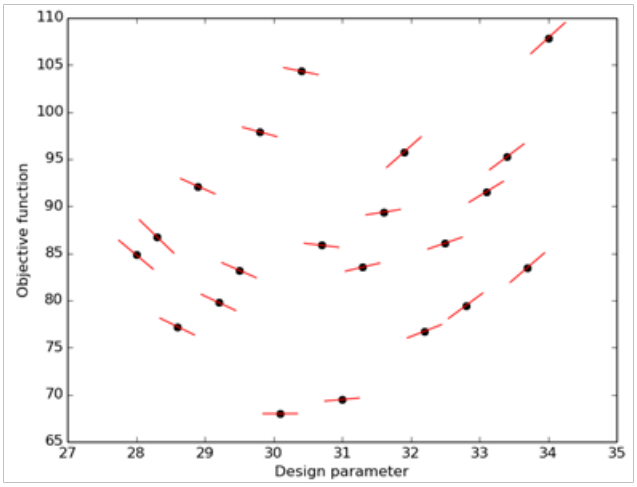

Figure 5. Least Squares Shadowing Gradient of Time-averaged $(z\text{-}28)^2$ in the Lorenz Attractor with Respect to r, for b = 8/3 and s=10, Computed on a Time Window of Length 5.

The Least Squares Shadowing method has developed a solid mathematical foundation in this project. It now has a rigorous convergence proof, achieved by combining dynamical system theory and numerical analysis. As the length of time averaging increases, not only does a time-averaged quantity converge to the infinite time average, but also its computed derivative converges to the derivative of the infinite time average. This convergence holds for the Least Squares Shadowing method but not for the conventional adjoint.

In this project, we successfully developed the Least Squares Shadowing method, an approach to overcome this difficulty of gradient computation in optimization of chaotic dynamical systems. The method is based on insight into the noise that pollutes the computed gradient. As can be illustrated with the sample in Figure 2, the noise in the gradient amplifies as two time series, each with a slightly different parameter, decorrelate from each other. In the simple example, the decorrelation is caused by taking independent samples. In a chaotic dynamical system, however, the decorrelation is caused by the butterfly effect, as illustrated in Figure 5. The key to solve this challenge is, therefore, finding trajectories that do not decorrelate from each other.

Trajectories of chaotic dynamical systems' sensitivity depend on both the parameters and initial conditions. The former means that by changing the parameters of the governing equation by a small amount, the new trajectory will grow further apart from the old one, even though they start from the same initial condition. This is similar to the latter sensitive dependence on initial conditions, which is better known as the "butterfly effect". It means that for chaotic systems, a small difference in the initial condition can result in a large difference later on.

To illustrate the similarity between the two sensitivities, we use the example of the Lorenz 63 system, a simplified Ordinary Differential Equation (ODE) model for atmospheric convection. It has three states x, y, z and parameter r. In Fig. 6, we show the sensitive dependence of trajectories on both the initial condition and the parameter. In the top row, we plot on the x-z plane 18 million trajectories with the

same initial condition but different r, uniformly distributed between 27 and 29. The value of r is colored by the spectrum of visible light. On the bottom row, we plot the same number of trajectories with the same parameter r = 28, but their initial conditions are uniformly distributed on a carefully chosen small line segment in the phase space. From left to right, Figure 6 shows snapshots at time 1.67, 5.0, 10.0, and 41.67, respectively. We observe many similarities and subtle differences between the effects of changing the parameter and those of changing the initial condition.

As we can see in the first three columns in Fig. 6, in the short time, changing the parameter results in diverging trajectories resembling the effect of only changing the initial condition; we call this the transient effect. In a long time, as shown in the last picture on the top row, changing the parameter results in a slightly shifted attractor, observable from the small color variation near the top and bottom in the top-right figure; we call this the long-time effect. The red shade on the upper rims and blue shade on the lower edges indicate that as we increase the value of r, the attractor moves up in the z-direction. This means that the time-averaged z has a positive and well-defined sensitivity to r.

The long-time effect of changing r is of importance for computing the long-time sensitivity; however, it is hidden under the diverging trajectories and is only visible after simulating an ensemble of millions of trajectories for a long time. The primary goal of Least Squares Shadowing is to subtract the transient effect from the effect of changing a parameter so that we can obtain the long-time sensitivity efficiently. In fact, the initial condition variation in the bottom row of Fig. 6 is obtained from a Least Squares Shadowing solution.

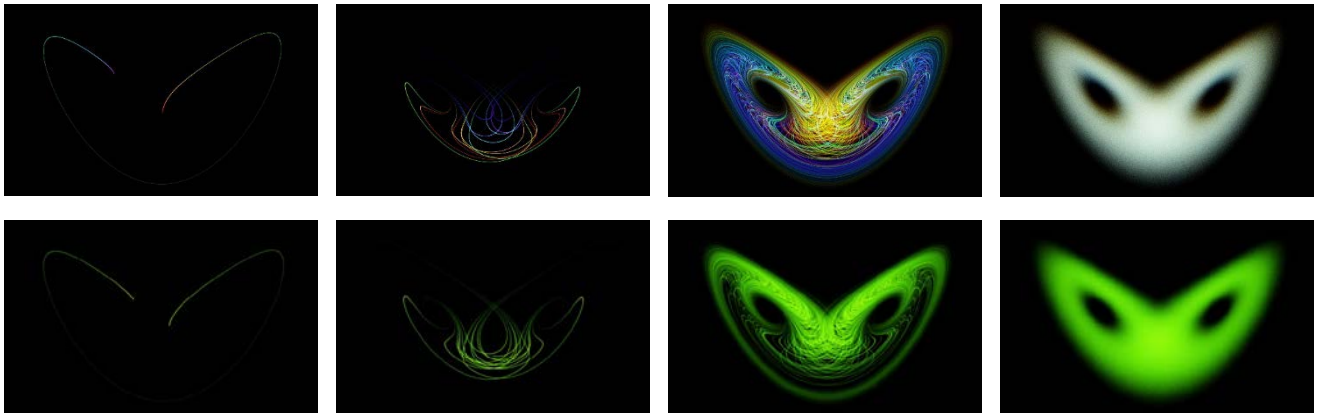

Figure 6. Snapshots of an Ensemble of 18 Million Trajectories of the Lorenz System.

The Non-Intrusive Least Squares Shadowing (NI-LSS) method constructs an initial condition perturbation whose transient effect is similar to a given parameter perturbation. This initial condition perturbation, under ergodicity assumption, has no impact on infinitely long time-averaged statistics. We, therefore, subtract the transient effect of this initial condition perturbation from the parameter perturbation, thereby distilling the long-time effect of a parameter perturbation.

Consider a dynamical system parameterized by a set of design variables, s:

$$\frac{du}{dt} = f(u, s)$$

with an initial condition u_0. Imposing it on an infinitesimal perturbation, δs in the parameter and δu_0 in the initial condition, increase the time derivative by an infinitesimal time-dependent factor $\delta\eta$. The new governing equation is

$$\frac{du'}{dt} = (1+\delta\eta)\, f(u', s+\delta s)$$

Note that $\delta\eta$ affects the rate of the time evolution of u' on its trajectory, but not the trajectory itself. By neglecting high order terms, the infinitesimal difference $\delta u \coloneqq u' - u$ satisfies the linearized equation:

$$\frac{d\delta u}{dt} = \partial_u f\, \delta u + \partial_s f\, \delta s + f\, \delta\eta$$

with an initial condition δu_0.

The idea of NI-LSS is to first solve the above equation with δu0=0 to obtain a solution $v = \delta u/\delta s$, then find a solution to $dw/dt = \partial_u f\, w + f\ \delta\eta$ with such initial condition and $\delta\eta$ that $v^* = v - w$ is removed of the transient effect, and only characterizes the motion of the attractor. Subtracting such w from v is the main idea behind NI-LSS. The criterion of a desired v* is that its long-time averaged magnitude, $\frac{1}{T}\int_0^T ||u^*||^2 dt$, is small. This allows us to compare states on the perturbed trajectory with states on the base trajectory, with them being close to each other.

The Non-Intrusive Least Squares Shadowing Algorithm

We assume that we have a tangent solver that operates on an existing nonlinear solution $u(t), t \in [0,T]$ in statistical equilibrium. It can solve either the inhomogeneous tangent equation $d\delta u/dt = \partial_u f\ \delta u + \partial_s f\ \delta s$ or the homogeneous tangent equation, $d\delta u/dt = \partial_u f\ \delta u$, starting from any given initial perturbation δu(t0) at any time $t_0 \in [0,T]$, and return the solution at any $t_1 \in [t_0, T]$. We also assume that we know the objective function, J(u, s), and the tangent solver can compute its perturbation over the time span [t0, t1]. Mathematically, the tangent solver can be represented as a function

$$\boldsymbol{T}(t_0, t_1, \delta u(t_0), \delta s) \to (\delta u(t_1), \delta J),$$

where the inputs t0 and t1 control the time domain of the solution, δu(t0) provides the initial condition, and δs can be used to select whether a homogeneous (δs = 0) or inhomogeneous tangent equation is solved. The output δu(t1) gives the solution at t1; $\delta J \coloneqq \partial_u J\ \delta u + \partial_s J$ is a function of t over [t0, t1], representing the perturbation in the objective function J(u, s).

The tangent NI-LSS algorithm runs this tangent solver $\boldsymbol{T}$ to compute the sensitivity derivative of the long time averaged objective function,

$$\frac{d\bar{J}(s)}{ds} \coloneqq \frac{d}{ds}\left\{\lim_{T\to\infty} \frac{1}{T}\int_0^T J(u,s)dt\right\}$$

1. Subdivide the interval $[0,T]$ into K time segments, $0 = T_0 < T_1 < \cdots < T_K = T$, such that the divergence of the tangent equation in each time segment $[T_k, T_{k+1}]$, due to the transient effect of the chaotic system, does not exceed O(10). This subdivision is to prevent numerical instability. The interrelationship among the subsequent steps of this algorithm can be visualized in Fig. 7.

2. Choose m orthonormal initial conditions for the homogeneous tangent equation, denoted as $w_0^i(T_0), i = 1, \dots, m$. Set the initial condition for the inhomogeneous tangent equation to $v_0(T_0) = 0$. These are the green blocks in Fig. 4.2. For $k = 0, \dots, K-1$, loop through Steps 4-6:
3. Run the inhomogeneous tangent solver (See Step 3 in Fig. 4.2):

$$\boldsymbol{T}(T_k, T_{k+1}, v_k(T_k), \delta s) \to \left(v_k(T_{k+1}), \delta J_k^0\right)$$

4. Run the homogeneous tangent solver m times (See Step 4 in Fig. 4.2):

$$\boldsymbol{T}\left(T_k, T_{k+1}, w_k^i(T_k), 0\right) \to \left(w_k^i(T_{k+1}), \delta J_k^i\right), \;\; i = 1, \dots, m$$

5. Orthonormalize $w_k^i(T_{k+1}), i = 1, \dots, m$. This is to construct an upper triangular matrix R_k (numerically through a QR factorization) and a vector ξ_k such that

$$w_k^i(T_{k+1}) + \xi_{k,i} f_{k+1} = \sum_{j=1}^{m} R_{k,ij} \cdot w_{k+1}^j(T_{k+1}),$$

and the resulting $w_{k+1}^i(T_{k+1}), i = 1, \dots, m$ are orthonormal to each other and orthogonal to $f_{k+1} \coloneqq f(u(T_{k+1}))$. See Step 5 in Fig. 4.2.

6. Orthogonalize $v_k(T_{k+1})$ with respect to each $w_{k+1}^i(T_{k+1}), i = 1, \dots, m$. This is to construct a vector b_k and scalar $\xi_{k,0}$ such that

$$v_{k+1}(T_{k+1}) + \xi_{k,0} f_{k+1} = v_k(T_{k+1}) - \sum_{j=1}^{m} b_{k,j} \cdot w_{k+1}^j(T_{k+1}),$$

and the resulting $v_{k+1}(T_{k+1})$ is orthogonal to each $w_{k+1}^i(T_{k+1}), i = 1, \dots, m$, as well as to f_{k+1}. See Step 6 in Fig. 4.2.

End of the k-loop started at Step 3.

7. Solve the reduced Least Squares Shadowing problem

$$\min_{a_{k,k=0,K-1}} \sum_{k=0}^{K-1} a_k^T a_k \quad s.t. \quad a_{k+1} = R_k a_k + b_k, \quad k = 0, \dots, K-2,$$

where the matrices R_k and vectors b_k are obtained from Steps 5 and 6; each $a_k = \left[a_k^1, \dots, a_k^m\right]^T$ in the solution is a vector of length m. See Step 7 in Fig. 4.2.

8. Compute the sensitivity derivative

$$\frac{d\bar{J}(s)}{ds} \approx \frac{1}{T} \sum_{k=0}^{K-1} \int_{T_k}^{T_{k+1}} \delta J_k(t) + \xi_k \left(J\left(u(T_{k+1})\right) - J\left(u(t)\right)\right) dt$$

where δJ_k and ξ_k are computed by combining the solution of Step 8 with results in Steps 4, 5, and 6:

$$\delta J_k = \delta J_k^0 + \sum_{i=1}^{m} a_k^i \, \delta J_k^i, \quad \xi_k = \xi_k^0 + \sum_{i=1}^{m} a_k^i \xi_k^i.$$

See Step 8 in Fig. 7.

It should be noted that this algorithm applies to both shape and sizing design variables in our proposed effort. Both types of design variables feed into Step 3, a tangent solver coupling the complex version of FUN3D and a discrete tangent solver of a 2-dof time-domain structural solver.

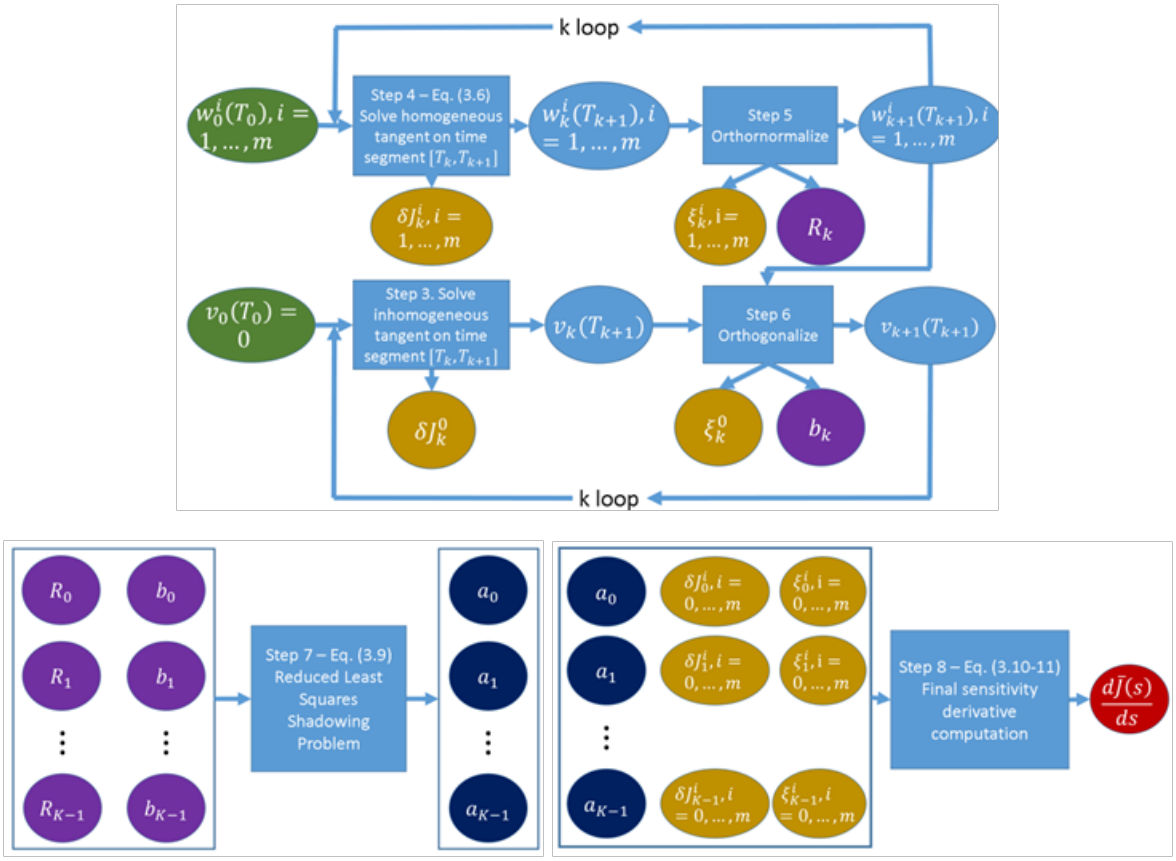

Figure 7. The Computational Diagram for the Tangent NI-LSS Algorithm.

Demonstration of the NI-LSS algorithm

In this project, we have not only developed the NI-LSS algorithm, proved its theoretical properties, but also have demonstrated its applicability in several computational fluid dynamics (CFD) problems.

Unsteady 2D laminar flow over stalled NACA 0012 airfoil at 20 degrees angle of attack.

This case is computed using FUN3D, a compressible flow solver developed at NASA Langley. The Reynolds number is 10,000. Sensitivity analysis is accomplished by coupling FUN3D with FDS, a computational tool developed in this project.

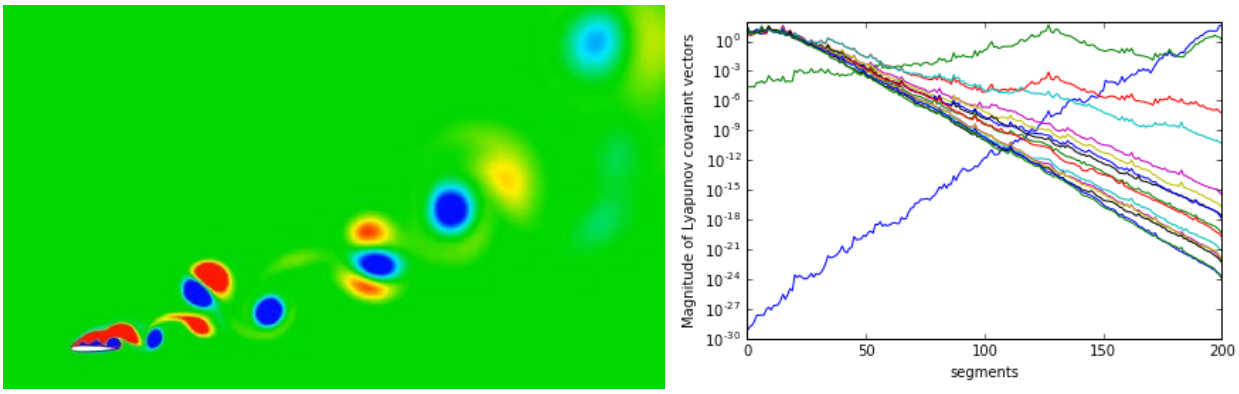

Figure 8. Left: Vorticity field of 2D laminar flow over a stalled NACA 0012 at 20 degrees angle of attack. Right: Magnitude of covariant Lyapunov vectors, two corresponds positive Lyapunov exponents; the rest correspond to negative ones.

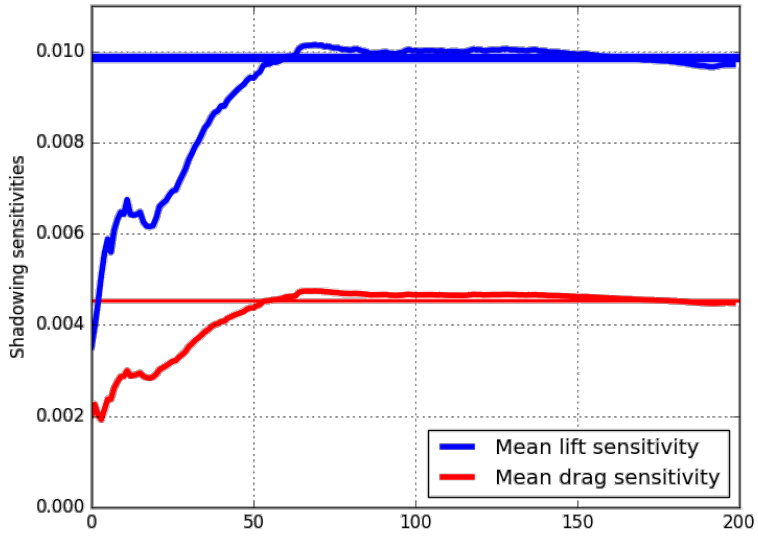

Figure 9. Convergence of the NI-LSS algorithm for computing the derivative of time-averaged lift and drag with respect the inflow Mach number.

Unsteady 2D internal laminar flow over a backward facing step

This case is computed using OpenFOAM, an open source flow solver. The Reynolds number is 1,000,000. Sensitivity analysis is accomplished by coupling OpenFOAM with FDS, a computational tool developed in this project.

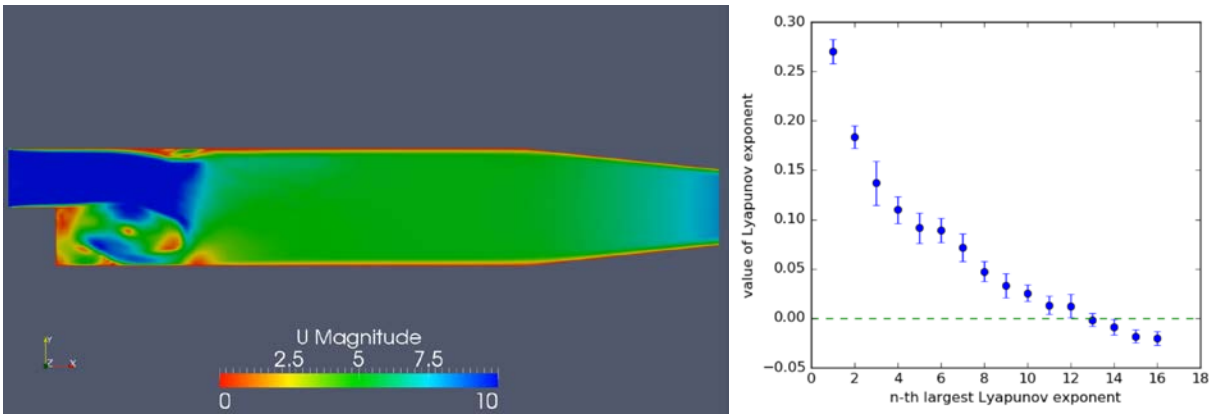

Figure 10. Left: Velocity field of 2D internal laminar flow over a backward facing step. Right: The computed largest Lyapunov exponents.

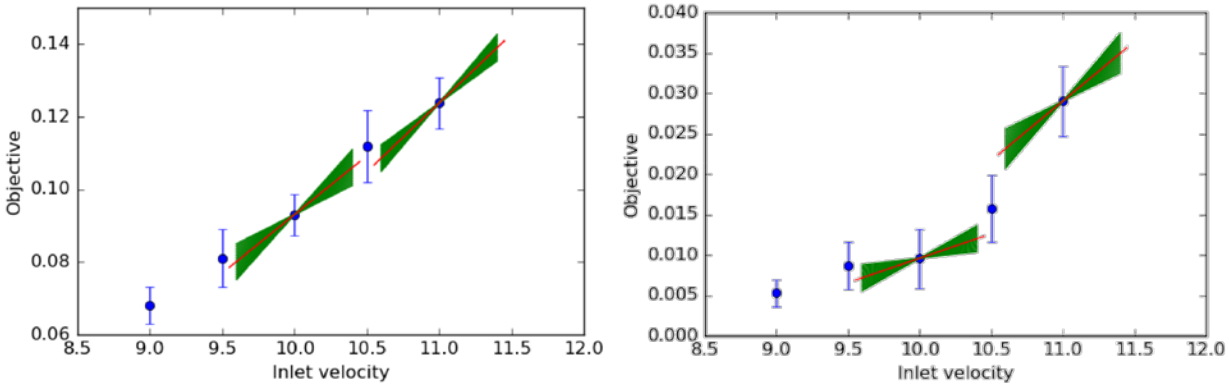

Figure 11. Sensitivities computed by NI-LSS compared to finite difference. The objective function is the time-averaged squared velocity (left) and time-averaged eight power of velocity (right) at a specific location in the flow field.

Unsteady 3D turbulent flow in a channel

This case is computed using EDDY, a high-order compressible flow solver developed at NASA Ames. The Reynolds number based on the friction velocity is 180. Sensitivity analysis is attempted by coupling EDDY with FDS, a computational tool developed in this project. The number of positive Lyapunov exponents, estimated to be about 1,200, is beyond the available computational resources. Sensitivity analysis is not accomplished in this project. A lower Reynolds number version of this problem, however, was later accomplished by Patrick Blonigan, a student supported by this project, after he graduated and hired by NASA Langley as a postdoc.

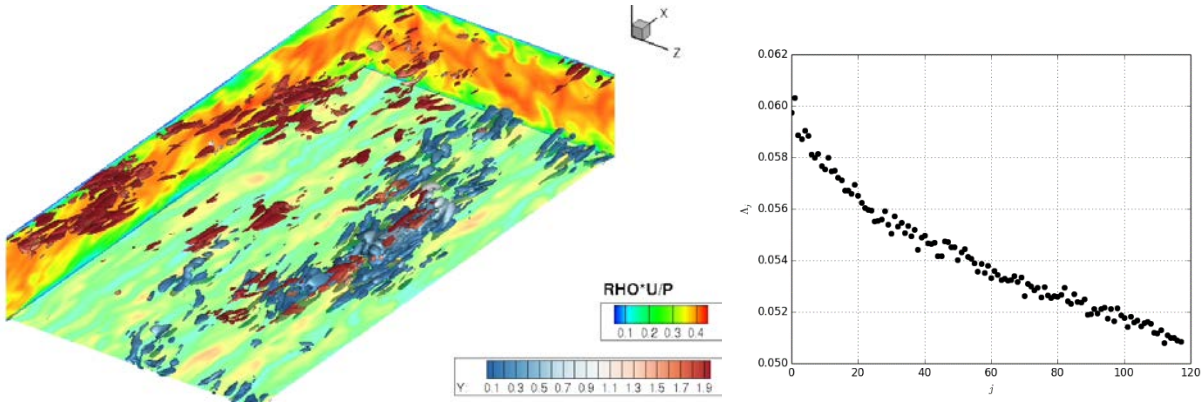

Figure 12. Left: Velocity and skin friction of a 3D turbulent channel flow overplayed with a covariant Lyapunov vector. Right: The computed largest Lyapunov exponents.

Unsteady 3D flow over a circular cylinder

This case is computed using CharLES, a compressible unsteady flow solver developed in the Center for Turbulence Research at Stanford and Cascade Technologies. The Reynolds number is 525. Sensitivity analysis is accomplished by coupling CharLES with FDS, a computational tool developed in this project.

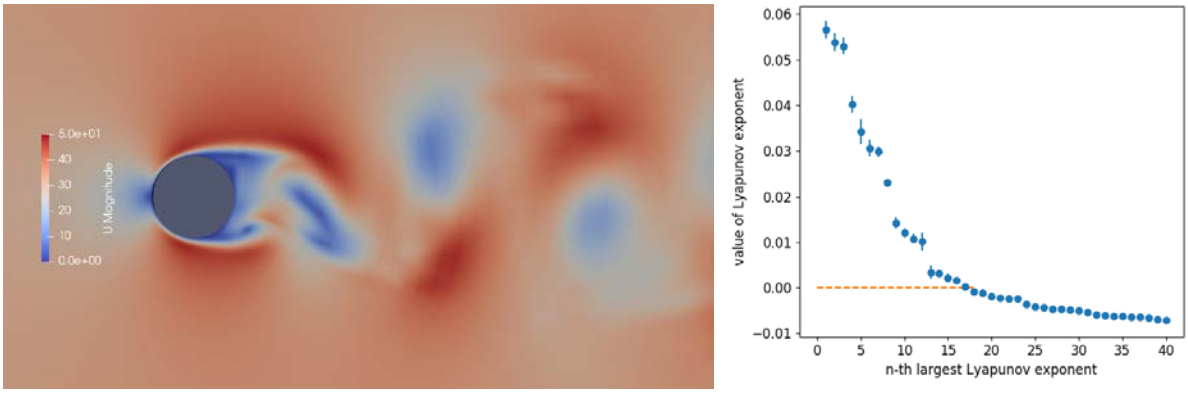

Figure 13. Left: Velocity and skin friction of a 3D flow over a circular cylinder. Right: The computed largest Lyapunov exponents.

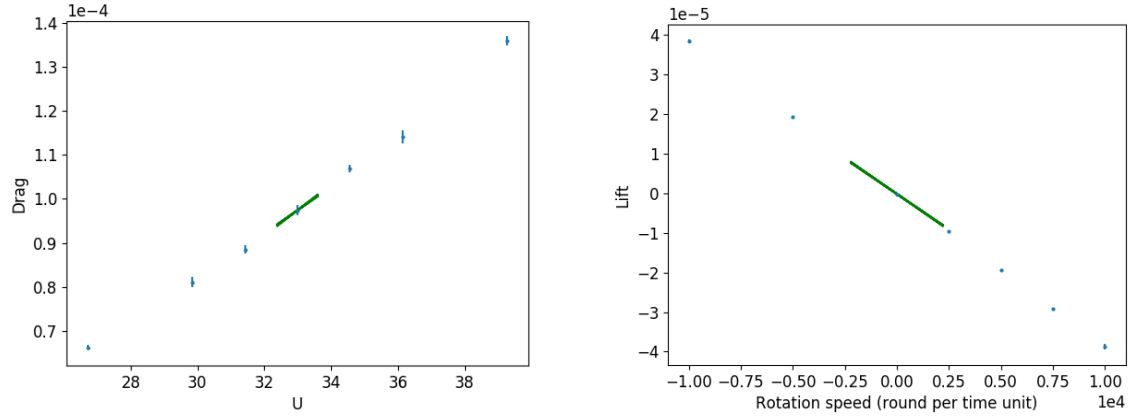

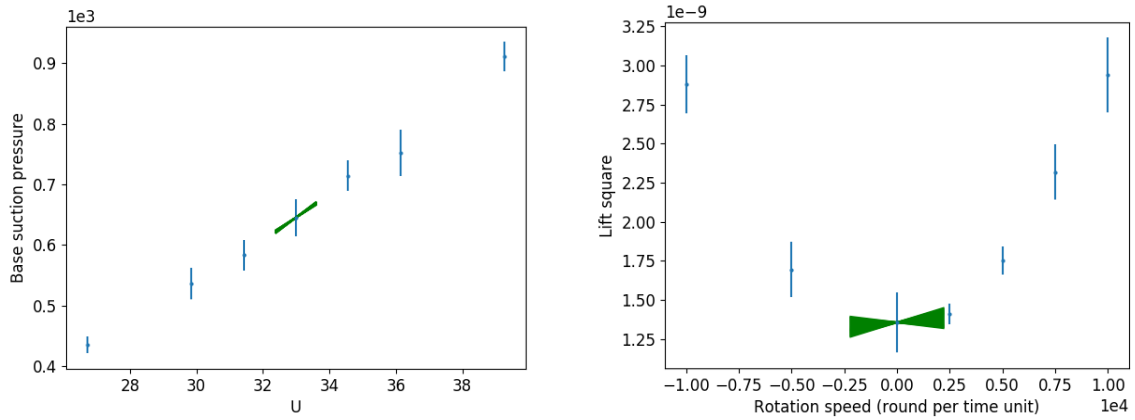

Figure 14. Sensitivities computed by NI-LSS compared to finite difference. The objective functions include the time averaged lift, drag, and pressure at the downstream point of the cylinder. The parameters include the inflow velocity and the rotation rate of the cylinder.

Students Supported

- Patrick Blonigan. Hired as a postdoc at NASA Ames, and then a staff scientist at Sandia National Labs after obtaining his PhD at MIT.
- Angxiu Ni. Currently a PhD student in mathematics at UC Berkeley.

Publications and Presentations

Journal publications

- Lyapunov spectrum of the separated flow around the NACA 0012 airfoil and its dependence on numerical discretization P Fernandez, Q Wang Journal of Computational Physics 350, 453-469
- Multiple shooting shadowing for sensitivity analysis of chaotic dynamical systems PJ Blonigan, Q Wang Journal of Computational Physics 354, 447-475
- Least Squares Shadowing method for sensitivity analysis of differential equations M Chater, A Ni, PJ Blonigan, Q Wang SIAM Journal on Numerical Analysis 55 (6), 3030-3046
- Least-Squares Shadowing Sensitivity Analysis of Chaotic Flow Around a Two-Dimensional Airfoil PJ Blonigan, Q Wang, EJ Nielsen, B Diskin AIAA Journal, 658-672
- Simplified Least Squares Shadowing sensitivity analysis for chaotic ODEs and PDEs M Chater, A Ni, Q Wang Journal of Computational Physics 329, 126-140
- A framework for simultaneous aerodynamic design optimization in the presence of chaos S Günther, NR Gauger, Q Wang Journal of Computational Physics 328, 387-398
- Simultaneous single-step one-shot optimization with unsteady PDEs S Guenther, NR Gauger, Q Wang Journal of Computational and Applied Mathematics 294, 12-22

Conference Presentations

- Least Squares Shadowing and Lyapunov Covariant Modes of a 3-D cylinder flow at Reynolds number 525 A Ni, Q Wang APS Division of Fluid Dynamics Meeting 2017
- Stability, receptivity and sensitivity of linear, periodic and chaotic flows: application to a thermoacoustic system L Magri, Q Wang APS Division of Fluid Dynamics Meeting 2017

- Sensitivity analysis of hydrodynamic chaos in combustion using NILSS-AD N Chandramoorthy, Q Wang, L Magri, SHK Narayanan, P Hovland APS Division of Fluid Dynamics Meeting 2017
- Lyapunov spectrum of scale-resolving turbulent simulations. Application to chaotic adjoints P Fernandez, Q Wang 23rd AIAA Computational Fluid Dynamics Conference, 2017
- An Analysis of the Ensemble Adjoint Approach to Sensitivity Analysis in Chaotic Systems N Chandramoorthy, P Fernandez, C Talnikar, Q Wang 23rd AIAA Computational Fluid Dynamics Conference, 2017
- A non-intrusive algorithm for sensitivity analysis of chaotic flow simulations PJ Blonigan, Q Wang, EJ Nielsen, B Diskin 55th AIAA Aerospace Sciences Meeting, 2017
- Lyapunov exponents, covariant vectors and shadowing sensitivity analysis of 3D wakes: from laminar to chaotic regimes Q Wang, G Rigas, L Esclapez, L Magri, P Blonigan APS Division of Fluid Dynamics Meeting 2016
- Lyapunov Exponents and Covariant Vectors for Turbulent Flow Simulations P Blonigan, S Murman, P Fernandez, Q Wang APS Division of Fluid Dynamics Meeting 2016
- Sensitivity analysis on chaotic dynamical system by Non-Intrusive Least Square Shadowing (NI-LSS) A Ni, P Blonigan, M Chater, Q Wang, Z Zhang 46th AIAA Fluid Dynamics Conference, 2016
- Sensitivity Analysis of Chaotic Flow around Two-Dimensional Airfoil P Blonigan, Q Wang, E Nielsen, B Diskin APS Division of Fluid Dynamics Meeting 2015